Hindawi
Journal of Nanomaterials
Volume 2017, Article ID 5204639, 10 pages
https://doi.org/10.1155/2017/5204639

Research Article

Effect of Precursor Concentration on Structural Optical and Electrical Properties of NiO Thin Films Prepared by Spray Pyrolysis

Rafia Barir,[1,2] Boubaker Benhaoua,[1] Soufiane Benhamida,[1,2] Achour Rahal,[1] Toufik Sahraoui,[3] and Rachid Gheriani[2]

[1]*Laboratory VTRS, Faculty of Exact Sciences, El Oued University, 39000 El Oued, Algeria*
[2]*Faculty of Mathematics and Material Sciences, University of Ouargla, 30000 Ouargla, Algeria*
[3]*Laboratoire de Microscopie Electronique & Sciences des Matériaux, USTO-MB, BP 1505 El MNaouer, Oran, Algeria*

Correspondence should be addressed to Boubaker Benhaoua; benhaouab@yahoo.fr

Received 1 February 2017; Accepted 11 April 2017; Published 10 May 2017

Academic Editor: Victor M. Castaño

Undoped nickel oxide (NiO) thin films were deposited on 500°C heated glass substrates using spray pyrolysis method at (0.015–0.1 M) range of precursor. The latter was obtained by decomposition of nickel nitrate hexahydrate in double distilled water. Effect of precursor concentration on structural, optical, and electrical properties of NiO thin films was investigated. X-ray diffraction (XRD) shows the formation of NiO under cubic structure with single diffraction peak along *(111)* plane at $2\theta = 37.24^{\circ}$. When precursor concentration reaches 0.1 M, an increment in NiO crystallite size over 37.04 nm was obtained indicating the product nano structure. SEM images reveal that beyond 0.04 M as precursor concentration the substrate becomes completely covered with NiO and thin films exhibit formation of nano agglomerations at the top of the sample surface. Ni-O bonds vibrations modes in the product of films were confirmed by FT-IR analysis. Transparency of the films ranged from 57 to 88% and band gap energy of the films decreases from 3.68 to 3.60 eV with increasing precursor concentration. Electrical properties of the elaborated NiO thin films were correlated to the precursor concentration.

1. Introduction

Transition metal oxides (TMOs) have attracted great attention in fundamental research field recently, because of their diverse physical properties, materials science, renewable energy, and microelectronics and nanotechnology fields applications [1–4]. They were used as light-emitting diodes (LEDs) [5], smart windows [6], and electrode material for Li-ion batteries [7]. Such metal oxides include semiconducting or metallic oxides like ZnO, TiO_2, NiO, Fe_2O_3, doped γ-Fe_2O_3, and Cr_2O_3 [8]. Due to its high excellent chemical stability nickel oxide (NiO) has received a great deal of interest. Besides its low cost and large specific capacitance, its optical, electrical, and magnetic properties made it as favorite candidate [9]. NiO is a very important VIII–VI semiconductor having NaCl-type structure [10]. It has wide band gap ranging from 3.6 to 4.0 eV [11]. Nonstoichiometric nickel oxide is a good p-type semiconductor owing to its defect structure [12]. It was shown that NiO thin films exhibit weak resistivity which maybe is due to the creation of nickel vacancies and interstitial oxygen atoms in their structures [13, 14].

In previous works different synthetic routes have been used for NiO thin films deposition including electron beam deposition [15], DC reactive sputtering [16, 17], thermal evaporation [18], Chemical Vapor Deposition [19], sol-gel technique [20], pulsed plasma deposition [21], and electrodeposition [22]. Among these, we will focus more particularly in this paper on the spray pyrolysis (SP) process, owing to its several advantages such as low cost of the apparatus, large area with high homogeneity, and easy control of structure of the deposited films [23–26].

In this paper, undoped NiO thin films were deposited on 500°C heated glass substrates using the spray pyrolysis

technique. Effects of precursor concentration on the structural and optical properties of NiO thin films are reported, discussed, and compared to results carried out in literature. Investigation of structural and optical properties, of obtained thin films, was done using X-ray diffraction (XRD), FT-IR, and UV-visible spectroscopy, whereas for electrical properties Seebek effect and four-point probe were processed on all the samples to affirm their p-type conductivity and to correlate it to the concentration of precursor.

2. Materials and Methods

2.1. Synthesis of Thin Films. NiO thin films were prepared from a solution of nickel nitrate hexahydrate [$Ni(NO_3)2$, $6H_2O$]. The precursor was dissolved in double distilled water with adding few drops of nitric acid (HNO_3) as stabilizer. The precursor concentration, which served as a starting solution, was varied from 0.015 to 0.1 M. The resulting solution was stirred at room temperature using a magnetic stirrer for half an hour to yield a clear and transparent solution. The obtained blend was used as a stock solution for spray pyrolysis. Microscopic glass slides (Ref 217102 with dimensions of 75 × 25 × 1.1 mm^3) were used as substrates. The later were cleaned with alcohol in an ultrasonic bath and distilled water then blow-dried with dry air. The heat temperature of the substrates was fixed at 500°C, the nozzle-substrate distance was kept 45 cm, the spray rate was 2 ml/min, and each spray takes one second, whereas the time interval between two successive sprays was 10 second to avoid the substrate temperature fall. Different concentrated solutions of fixed volume (40 ml) were sprayed separately on heated glass substrates leading to undoped NiO thin films. After deposition, the films were allowed to cool till room temperature.

2.2. Thin Films Characterization. Structural characterizations are carried out using X-ray diffraction (XRD) with an X-ray diffractometer (BRUKER-AXS type D8) equipped with X'Pert High Score under Cu Kα (λ = 1.5406 Å) radiation whereas the scanning range of (2θ) was between 30° and 55°. Bonding information was obtained by Fourier transformed infrared (FT-IR) spectroscopy apparatus (Shimadzu IR-Infinity1); the scan of the measurements ranged from 400 to 4000 cm^{-1}. Optical transmittance of the deposited thin films was measured in the range of 300–900 nm by using an UV-visible spectrophotometer (SHUMATZU 1800). To affirm the p-type conductivity and its variation with precursor concentration, Seebek effect and four-point probe were processed on sheets having 2 × 1 cm^2 for all the samples. The measurement of the thickness (t) was done by gravimetric weight difference method, by assuming constant density of NiO as 6.7 gm/cm^3. The film thickness t is given by [50]

$$t = \frac{\Delta m}{\rho A}, \tag{1}$$

where Δm is the difference in mass before and after deposition, ρ is the bulk density, and A is the area of the film.

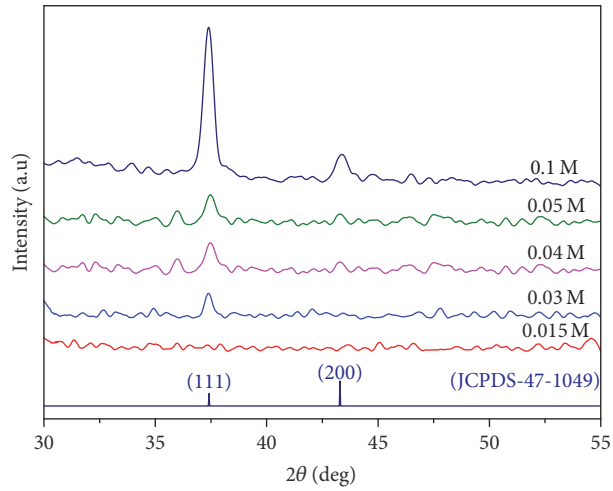

Figure 1: X-ray patterns of NiO. Thin films prepared at 500°C with different precursor concentration.

3. Results and Discussion

3.1. Structural Properties

3.1.1. X-Ray Diffraction. X-ray diffraction (XRD) patterns of NiO thin films elaborated by the spray pyrolysis were recorded for different precursor concentration as 0.015, 0.03, 0.04, 0.05, and 0.1 M and shown in Figure 1. The as-deposited thin film at 0.015 M shows an amorphous structure in nature; it indicates the poor crystallinity of the film. This may be due to the incomplete formation of the NiO film at this concentration [51]. With increasing of precursor concentration from 0.03 to 0.05 M, the commencement of crystallization was observed. It is seen from XRD patterns that only single peak appears at 2θ = 37.24°, which is attributed to the *(111)* diffraction peak and clearly indicated that the NiO phase exists under its face centered cubic (fcc) structure, which is in good agreement with Joint Committee on Powder Diffraction Standards (JCPDS card number 47-1049) [52]. From XRD patterns, with respect to limit detection, no other impurity peaks were detected. The thin film that can be seen, deposited at 0.1 M, has higher and sharper *(111)* diffraction peak indicating an improvement in crystallization of this film compared to other ones deposited at lower concentrations. It is worth noting that other peaks at (200) appeared in films when the concentration of solution exceeds 0.03 M. In order to obtain more structural information, different structural parameters such as lattice constants a, interplanar spacing d_{hkl}, grain size D, mean strain ε, and dislocation density δ of NiO thin films coated on various precursor concentration are calculated. In the case of cubic structure, the lattice constant a for NiO a phase is calculated using the following equation [53]:

$$d_{hkl} = \frac{a}{\sqrt{h^2 + k^2 + l^2}}, \tag{2}$$

where hkl are Miller indices and d_{hkl} is the interplanar spacing given by Bragg's law [54]:

$$2d_{hkl} \sin\theta = n\lambda, \tag{3}$$

Table 1: Values of Bragg angle 2θ, lattice constants a, full width at half maximum β, grain size G, mean strain ε, and dislocation density δ deduced from the (111) peak of NiO thin films prepared at 500°C with different of precursor concentration.

Precursor concentration	2θ (deg)	Lattice constants (Å)	β (deg)	D (nm)	E (%)	$\delta \times 10^{15}$ (lines /m^2)
0.015 M	—	—	—	—	—	—
0.03 M	37.396	4.160	0.576	15.207	−0.397	4.323
0.04 M	37.377	4.163	0.432	20.275	−0.313	2.432
0.05 M	37.496	4.153	0.472	18.552	−0.562	2.905
0.1 M	37.392	4.165	0.236	37.085	−0.284	7.271

where n is the order of diffraction taken equal unity (first order), λ is the wavelength of the radiation (λ = 1.54056 Å) for CuKa radiation, and θ is the Bragg diffraction angle of peak in degree. The grain size D of the films was calculated for *(111)* plane by using Scherrer's equation [55]:

$$D = \frac{0.9\lambda}{\beta \cos\theta}, \quad (4)$$

where β is the full width at half maximum (FWHM) corresponding to diffraction angle θ and λ is the X-ray wavelength of the incident radiation (1.54056 Å).

The mean strain ε in NiO thin films can be estimated via the formula [56]

$$\varepsilon = \left(\frac{a - a_0}{a_0}\right) \times 100\%, \quad (5)$$

where a and a_0 are the lattices constants of NiO thin films and the standard lattice constant of the bulk material (a_0 = 4.1769 Å) according to standard card (JCPDS, number 47-1049).

The dislocation density δ, which is defined as the dislocation line per unit volume, has been calculated using the following relation [57]:

$$\delta = \frac{1}{D^2}. \quad (6)$$

Table 1 summarizes variations of different structural parameters of elaborated NiO thin films with various precursor concentrations. Variation of grain size along the *(111)* plan as a function of precursor concentration is reported in Figure 2. As can be seen from this figure when precursor concentration covers the average 0.03–0.1 M, the grain sizes of the thin films were about 15.20, 20.27, 18.55, and 37.08 nm for samples deposited using 0.03 M, 0.04 M, 0.05, and 0.1 M, respectively. The film prepared at 0.1 M concentration presents the high value of grain size (37.08 nm) revealing the nano structure of the product. The increase in the grain size indicates a decrease in the lattice defects, which in turn reduces internal strain and dislocation density [58] as it was seen in Table 1.

3.1.2. SEM Images. Figures 3(a)–3(d) represent the surface morphologies of the samples with different concentration of the precursor (0.015–0.1 M). As can be seen thin film elaborated with 0.015 M precursor concentration reveals that NiO mater starts to grow on the substrate but the latter is not well covered. At 0.03 M precursor concentration thin films continues to grow and exhibits discontinued microplots on the surface of the substrate (see Figure 3(b)). With increasing precursor concentration to 0.04 M the substrate becomes well covered with presence of nanoagglomerations along the entire surface of the substrate as seen in Figure 3(c). Beyond 0.04 M as precursor concentration the substrate becomes completely covered with NiO and thin films showing that nanoagglomerations continue its formation to becoming microagglomerations at the top of the sample surface; see, for instance, Figure 3(d).

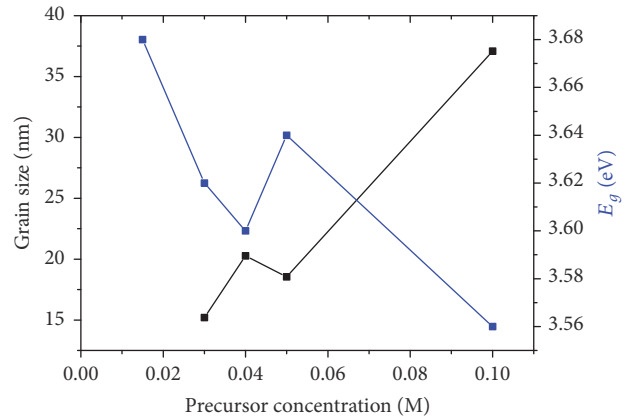

Figure 2: Variations of grain size and band gap (E_g) of NiO thin films as function of precursor concentration prepared at 500°C.

3.1.3. Fourier Transform Infrared (FT-IR) Analysis. To further support the XRD results, the quality and composition of elaborated NiO thin films were investigated by FT-IR spectroscopy. Analysis through FT-IR spectroscopy was done because its spectra are powerful tool to provide information on the nature of obtained metal oxides. In general oxides and hydroxides of metal nanoparticles give absorptions peaks in wave number region below 1000 cm^{-1} that arises from interatomic vibrations [32, 59, 60]. Figures 4(a)–4(e) show the FT-IR spectrum of NiO thin films with varying precursor concentration from 0.015 to 0.1 M, respectively. As indicated in the spectra, for all samples characteristics peaks at 407, 437, 475, 500, 520, 560, 607, 668, and 820 cm^{-1} correspond to Ni-O stretching vibration bonds as reported in literature [29, 34, 35] but with use of others deposition methods. Table 2 summarizes obtained results in this study in agreement with other results carried out in literature [27–49, 52].

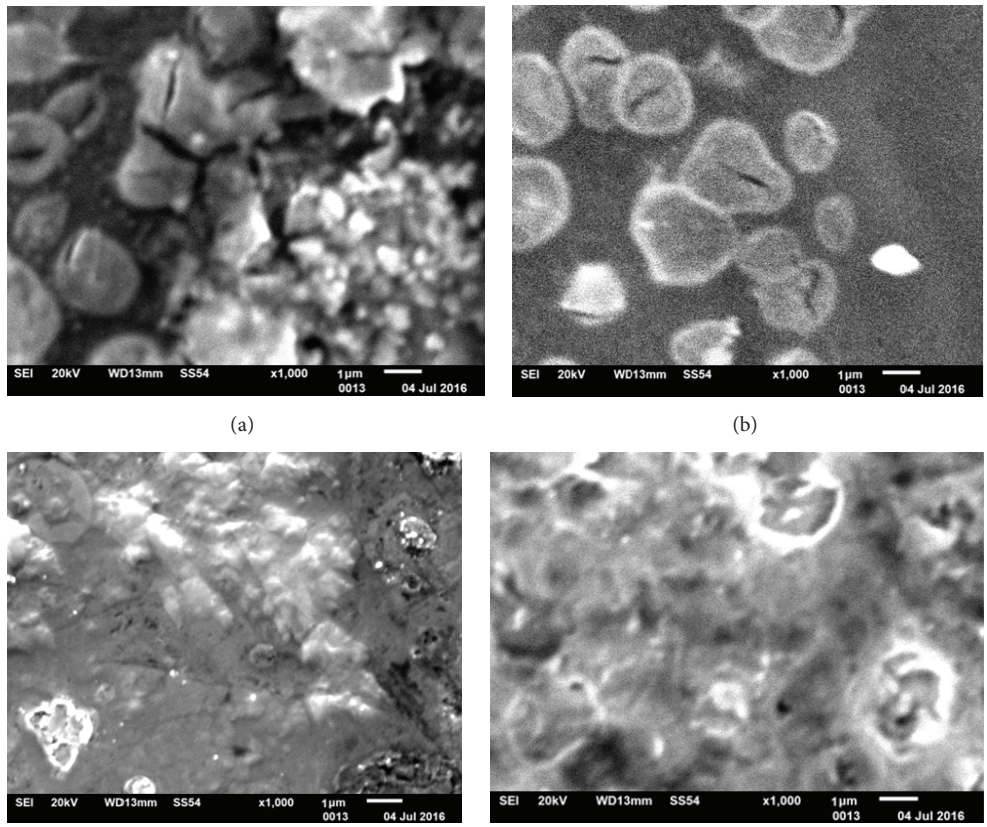

Figure 3: *SEM Images* of NiO thin films prepared at 500°C with different precursor concentration, (a) samples prepared with 0.015, (b) with 0.03, and (c) with 0.04 M, (d) with 0.1 M.

Table 2: The assignments of the most important bands in the FT-IR spectra of NiO thin films sprayed at 500°C with different of precursor concentration.

Samples	Positions (cm^{-1}) in this work in respect to the concentration	Assignments	Positions (cm^{-1}) in other works
0.015, 0.03 and 0.04 M	**(409), (411), (412)**	Nickel-oxygen interaction	**410** [27, 28]
	(475), (474)	Ni-O stretching vibration	**474.5-475-475** [29–31]
	(545), (550), (556)	bands metal- oxygen vibrations-stretching	**450-550** [32], **450-560** [33], **552** [34],
	(605), (606)	Ni-O-H stretching band	**607-619** [35, 36]
	(643-669), (641-668), (641)	Ni-O stretching vibration	**600-700** [37], **660** [38], **663** [39]
	(779-756-723), (778-754-722),	Mode bending modes O-M-O	**400-820** [34], **400-850** [40]
0.05 and 0.1 M	**(407), (418)**	Nickel-oxygen interaction	**410, 413** [27, 28, 41]
	(437), (437)	Ni-O Absorption band	**435.93-437** [29, 42]
	(466-542-564), (458-480)	Bond stretching vibration Ni-O	**450-560** [33], **460** [43], **445-490** [44], **470** [35, 45],
	(511), (—)	Bending modes O-M-O	**400-500** [46]
	(520), (520)	Nickel-oxygen stretch	**520-520-524** [47–49]
	(—), (566-596)	vibrations Ni-O bond	**660** [37], **663** [38]
	(608-690), (624-696-671)	band Ni-O-H stretching Bending between Ni and O	**607** [35], **600-700** [37], **624** [34],
	(723-790-820), (720-754-794-820)	Mode bending modes O-M-O	**400-820** [34], **400-850** [40]

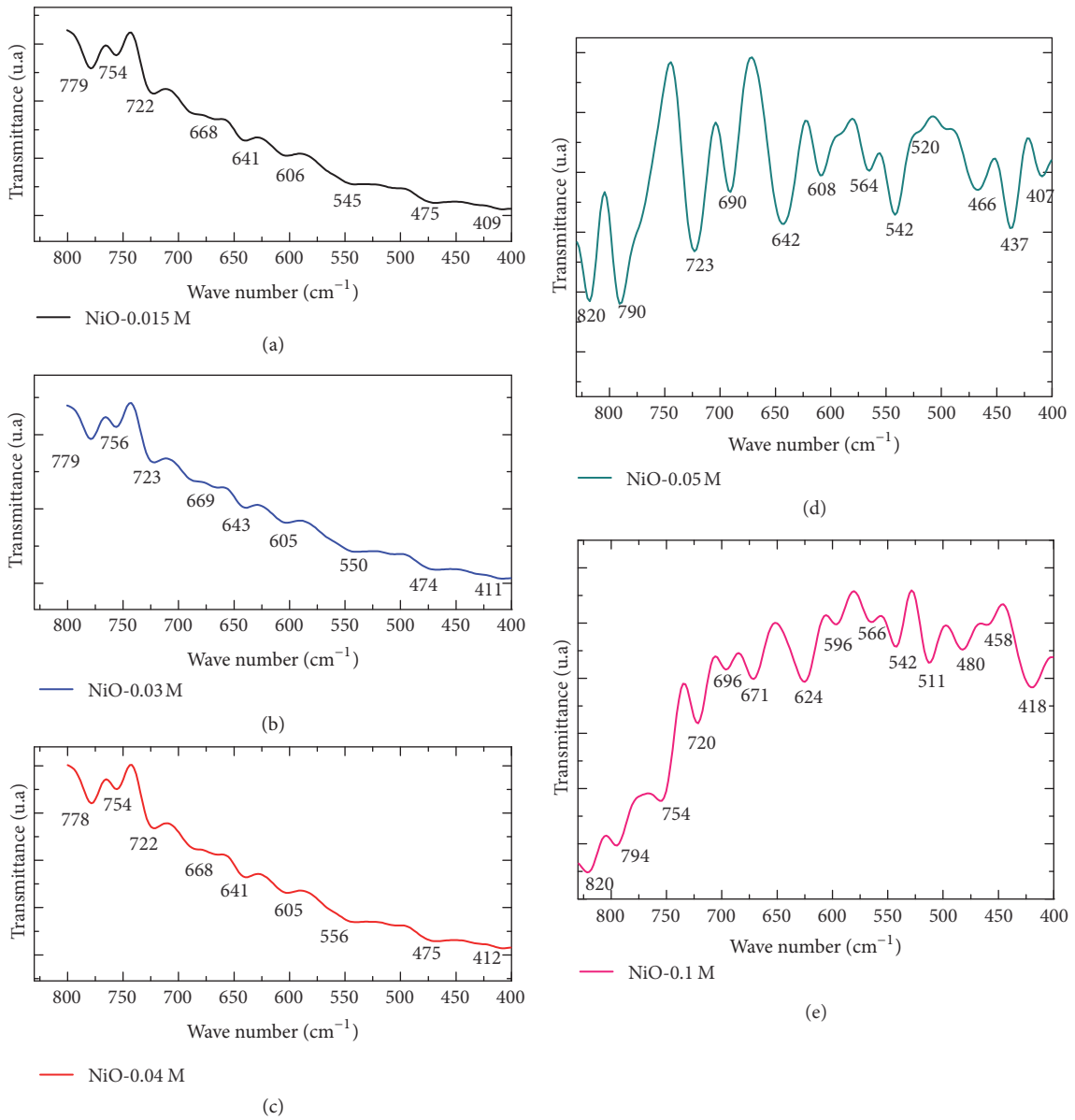

FIGURE 4: FT-IR spectra of NiO thin films prepared at 500°C with different precursor concentration, (d, e) samples prepared with 0.05 and 0.1 M, (a, b, c) with 0.015, 0.03, and 0.04 M.

To give confirmation to the observed 820 cm^{-1} absorption strength vibration, in the case of 0.05 and 0.1 M sprayed sample (Figures 4(d) and 4(e)), calculated wave number (in cm^{-1} as units) using Hook's law in simple harmonic oscillator model was done. As well known, Hook's law is illustrated by the following formula [61]:

$$\nu = \frac{1}{2\pi c}\sqrt{\frac{k}{\mu}}, \tag{7}$$

where c is the light velocity, k is the bond force constant, and μ is the reduced mass. Thus the position of specific band absorption of nickel oxide powders is determined on the basis of the bond force constant k ($= 5 \cdot 10^5$ dyne·cm^{-1}) and the reduced mass μ ($\mu = 1/m_{Ni} + 1/m_O$). This formula yields to theoretical NiO stretching vibration equal to 821 cm^{-1} which is closely equal to the observed 0.05 and 0.1 M sprayed samples, as seen in Figures 4(d) and 4(e), and corresponds to the bulk Ni-O vibration mode.

3.2. Optical Properties. Figure 5 shows the optical transmittance spectra recorded in the wave length range 300–900 nm. For all thin films prepared at various precursor concentrations, spectra show two regions: the first one at wavelength higher than 400 nm showing practically an average transmission between 57 and 88% and revealing a decrease by increasing the precursor concentrations and, based on calculated film thickness (t), transparence was found to be depending on thickness of samples reveling Beer-Lambert low as it was

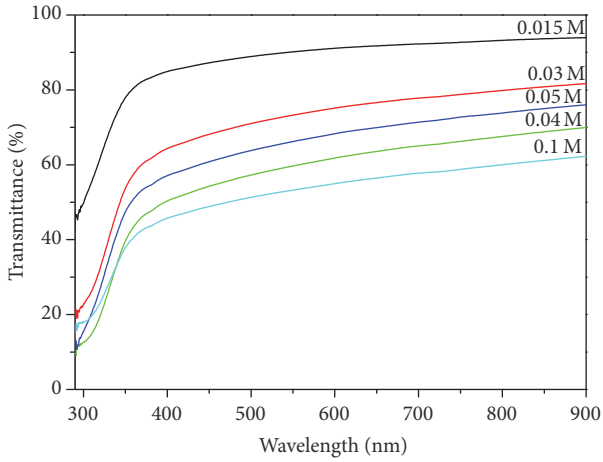

Figure 5: Spectral transmittance plots of NiO thin films prepared at 500°C with different precursor concentration.

Table 3: Values of thickness t, average transmittance, optical band gap energy E_g, and Urbach energy E_u of NiO thin films prepared at 500°C with different of precursor concentration.

Precursor concentration (M)	Thickness t (nm)	Average transmittance (%)	Gap energy E_g (eV)	Urbach energy E_u (meV)
0.015	181.57	88.30	3.68	309.40
0.03	191.66	71.01	3.62	365.76
0.04	170.36	57.56	3.60	394.36
0.05	190.34	64.28	3.64	400.16
0.1	200.00	51.66	3.56	453.72

shown in Table 3. The second region is at wavelength lower than 400 nm for which transparence decreases rapidly for all samples exhibiting the onset fundamental absorption due to the transition between the valence band and the conduction band [62].

For more investigation, absorption coefficient (α) of the NiO thin films was determined from the transmittance measurements using Swanepoel's method [63, 64]:

$$\alpha = \frac{1}{t} \ln\left(\frac{1}{T}\right), \tag{8}$$

where t and T are the thickness and transmittance of the film, respectively. Energy gap values depend in general on the films crystal structure (disorder and its regularity) [65]. Also (α) and the incident photon energy ($h\nu$) are related each other as they are given in Tauc's equation [66]:

$$(\alpha h\nu) = A\left(h\nu - E_g\right)^n, \tag{9}$$

where A is a constant, E_g is the band gap of the material, and n is an exponent which depends on the type of transition; $n = 1/2$; 2; 3/2; and 3 correspond to allowed direct, allowed indirect, forbidden direct, and forbidden indirect, respectively. Direct energy gap was determined by plotting a graph between $(\alpha h\nu)^2$ versus $h\nu$ and extrapolation of straight

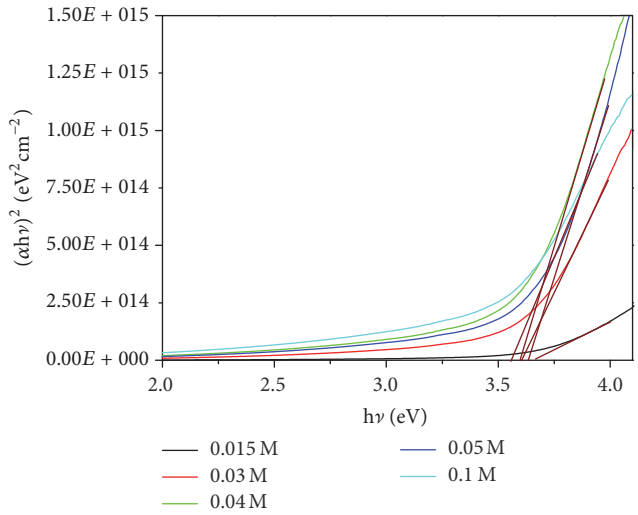

Figure 6: Band gap (E_g) estimation from Tauc's relation of NiO thin films prepared at 500°C with different of precursor concentration.

line to $(\alpha h\nu)^2 = 0$ gives the direct band gap values of different concentrated sprayed NiO thin films as seen in Figure 6. The calculated band gap values are listed in Table 3. Obtained band gap values are in good agreement with results carried out in literature [67, 68]. A disorder, so called Urbach tails, which is related to width of the localized states available in the optical band gap of the NiO thin films and affected its structure, was done for further investigation. This width, of the localized states, is related directly to a similar exponential tail for the density of states near band edges and can be expressed by the following relation [69]:

$$\alpha = \alpha_0 \exp\left(\frac{h\nu}{E_u}\right), \tag{10}$$

where $h\nu$ is the photon energy, α_0 is constant, and E_u is the Urbach energy which refers to the width of the exponential absorption edge. Figure 7 shows the variation of $\ln \alpha$ versus photon energy ($h\nu$) for the films. E_u values were calculated from reciprocal of the straight line slopes, as shown in the Figure 7, and illustrated in Table 3. As can be seen from Table 3, the energy band gap is averaged in 3.68–3.60 eV. The decrease in the optical band gap with precursor concentration may be attributed to the increase in grain size and decrease in structural disorder in the films as observed from Urbach energy analysis. In general it was shown that the band gap of all samples is inverted to Urbach energy [70] and the grain size is in respect to equation

$$\Delta E = E_{gn} - E_{gb} = \frac{\hbar^2 \pi^2}{m^*} \frac{1}{R^2} \tag{11}$$

driven from the well known formula given by the following relation [71]:

$$\Delta E = \left(E_{gb}{}^2 + \frac{2\hbar^2 \pi^2}{m^* R^2}\right)^{1/2}; \tag{12}$$

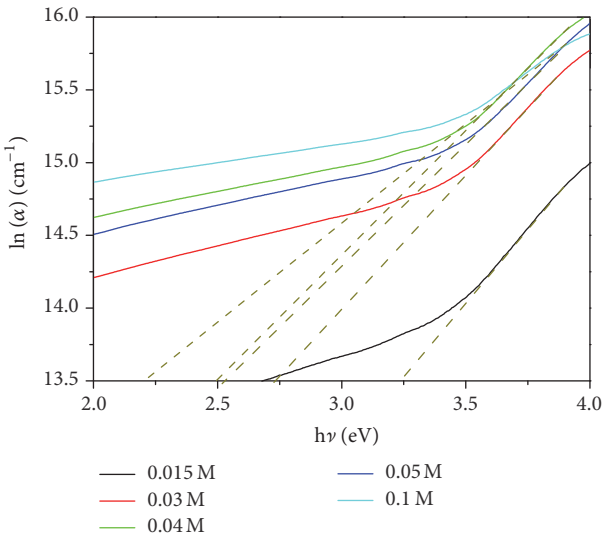

FIGURE 7: Variation of band gap (E_g) and Urbach energy (E_u) of NiO thin films as function of precursor concentration of NiO thin films prepared at 500°C.

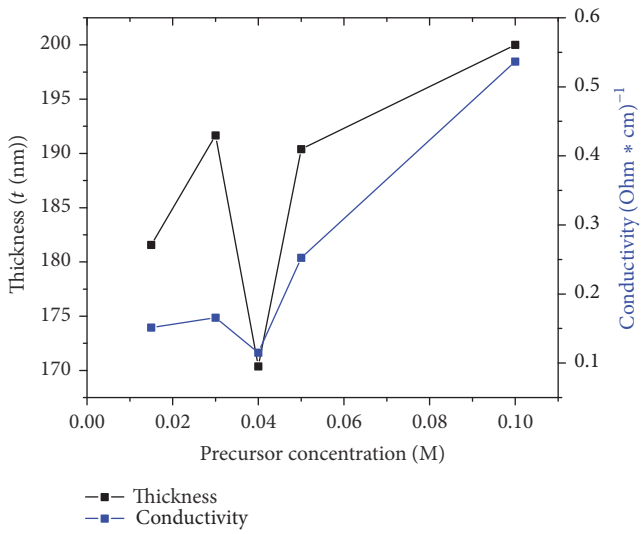

FIGURE 8: Variations of conductivity and thickness (t) of NiO thin films as function of precursor concentration prepared at 500°C.

this relation can be rewritten as follows:

$$E_{gn} = E_{gb}\left(1 + \frac{2\hbar^2\pi^2/m^*}{E_{gb}R^2}\right)^{1/2}, \quad (13)$$

where E_{gn} is the band gap of the film, E_{gb} is the band gap of bulk form of the material, and m^* and R are the electron effective mass and the radius of the nanocrystallites (or grains). Also this relation can be expanded as a series by neglecting the higher order of terms (since $(2\hbar^2\pi^2/m^*)/E_{gb}R^2 \ll 1$) yielding to the final expression, cited above, giving the variation of E_g as function of radius of crystallite size and confirms what is found in this study and observed from Figure 2.

3.3. Electrical Properties. It is worth noting that NiO is known as a p-type semiconductor due to the Ni^{+2} vacancies which is the considered defect for its p-type conductivity [11, 72]. Seebek effect was processed on all the samples and confirmed their p-type conductivity. The room temperature electrical conductivity (σ) was calculated using four-point probe. Figure 8 represents the electrical conductivity and the film thicknesses plotted as function of the precursor concentration; as can be seen from this plot the conductivity of the NiO thin films decreases from 0.16 Ω^{-1} cm^{-1} for thin film deposited with 0.015 M to a feeble value (0.11 Ω^{-1} cm^{-1}) at 0.04 M then increases to reach 0.53 Ω^{-1} cm^{-1} at 0.1 M. The electrical conductivity (σ) was correlated to the film thicknesses revealing the same behavior upon the precursor concentration.

4. Conclusions

Undoped nickel oxide (NiO) thin films were deposited on 500°C heated glass substrates using spray pyrolysis method. The NiO thin films were deposited with 0.015–0.1 M range of precursor concentration by decomposition of nickel nitrate hexahydrate [$Ni(NO_3)_2{\cdot}6H_2O$] in double distilled water. Structural studies using X-ray diffraction (XRD) show when precursor concentration is over 0.015 M formation of NiO under cubic structure with single diffraction peak along *(111)* plane at $2\theta = 37.24°$. Furthermore *(111)* peak intensity becomes more significant, when precursor concentration reaches 0.1 M, leading to an increment in NiO crystallite size close to 37 nm indicating nanosize structure of the films. SEM images reveal that beyond 0.04 M as precursor concentration the substrate becomes completely covered with NiO and thin films exhibit formation of nano agglomerations at the top of the sample surface. FT-IR analysis of spectra confirmed the existence of Ni-O bonds vibrations modes in the composition of product. Transmittance spectra showed that transparency of the films ranged from 57 to 88% and band gap energy of the films decreases from 3.68 to 3.60 eV with increasing precursor concentration whereas their thickness averaged from 170 to 210 nm. The electrical conductivity (σ) of the elaborated NiO thin films, having p-type character, was correlated to the film thicknesses revealing the same behavior upon the precursor concentration.

Conflicts of Interest

The authors declare that they have no conflicts of interest.

Acknowledgments

This work was supported in part by VTRS laboratory of El Oued University. X-ray diffraction data in this work were acquired with an instrument supported by the University of Biskra. The authors thank Dr. S. Benramache and B. Gasmi (Biskra University) for the assistance in XRD data acquisition.

References

[1] K. H. Krishna, O. M. Hussain, and C. Guillen, "Photo- and electrochromic properties of activated reactive evaporated," *Research Letters in Nanotechnology*, vol. 2008, pp. 1–5, 2008.

[2] J. Wu, Q. Wang, A. Umar et al., "Highly sensitive p-nitrophenol chemical sensor based on crystalline α-MnO_2 nanotubes," *New Journal of Chemistry*, vol. 38, no. 9, pp. 4420–4426, 2014.

[3] A. A. Demkov, P. Ponath, K. Fredrickson et al., "Integrated films of transition metal oxides for information technology," *Microelectronic Engineering*, vol. 147, article no. 9913, pp. 285–289, 2015.

[4] Z. He and X. Wang, "Renewable energy and fuel production over transition metal oxides: the role of oxygen defects and acidity," *Catalysis Today*, vol. 240, pp. 220–228, 2015.

[5] J.-M. Caruge, J. E. Halpert, V. Bulović, and M. G. Bawendi, "NiO as an inorganic hole-transporting layer in quantum-dot light-emitting devices," *Nano Letters*, vol. 6, no. 12, pp. 2991–2994, 2006.

[6] G. Bodurov, T. Ivanova, and K. Gesheva, "Technology and application of transition metal oxide of WVO as functional layers and NiO thin films as counter electrode material in electrochromic "Smart Windows"," *Physics Procedia*, vol. 46, pp. 149–158, 2013.

[7] Y. Wang, Y.-F. Zhang, H.-R. Liu, S.-J. Yu, and Q.-Z. Qin, "Nanocrystalline NiO thin film anode with MgO coating for Li-ion batteries," *Electrochimica Acta*, vol. 48, no. 28, pp. 4253–4259, 2003.

[8] C. Wang, L. Yin, L. Zhang, D. Xiang, and R. Gao, "Metal oxide gas sensors: sensitivity and influencing factors," *Sensors*, vol. 10, no. 3, pp. 2088–2106, 2010.

[9] A. Rengaraj, Y. Haldorai, C. H. Kwak et al., "Electrodeposition of flower-like nickel oxide on CVD-grown graphene to develop an electrochemical non-enzymatic biosensor," *Journal of Materials Chemistry B*, vol. 3, no. 30, pp. 6301–6309, 2015.

[10] J. C. Osuwa and G. I. Onyejiuwa, "Effects of variations in annealing temperature and annealing time on the spectral and solid state properties of nickel oxide (NiO) thin films," *Advanced Materials Research*, vol. 787, pp. 262–268, 2013.

[11] S. Nandy, B. Saha, M. K. Mitra, and K. K. Chattopadhyay, "Effect of oxygen partial pressure on the electrical and optical properties of highly (200) oriented p-type Ni_{1-x} O films by DC sputtering," *Journal of Materials Science*, vol. 42, no. 14, pp. 5766–5772, 2007.

[12] H.-L. Chen, Y.-M. Lu, and W.-S. Hwang, "Characterization of sputtered NiO thin films," *Surface and Coatings Technology*, vol. 198, no. 1–3, pp. 138–142, 2005.

[13] P. Puspharajah, S. Radhakrishna, and A. K. Arof, "Transparent conducting lithium-doped nickel oxide thin films by spray pyrolysis technique," *Journal of Materials Science*, vol. 32, no. 11, pp. 3001–3006, 1997.

[14] L. De Los Santos Valladares, A. Ionescu, S. Holmes et al., "Characterization of Ni thin films following thermal oxidation in air," *Journal of Vacuum Science & Technology B, Nanotechnology and Microelectronics: Materials, Processing, Measurement, and Phenomena*, vol. 32, no. 5, Article ID 051808, 2014.

[15] M. M. El-Nahass, M. Emam-Ismail, and M. El-Hagary, "Structural, optical and dispersion energy parameters of nickel oxide nanocrystalline thin films prepared by electron beam deposition technique," *Journal of Alloys and Compounds*, vol. 646, Article ID 34377, pp. 937–945, 2015.

[16] A. Karpinski, A. Ferrec, M. Richard-Plouet et al., "Deposition of nickel oxide by direct current reactive sputtering: effect of oxygen partial pressure," *Thin Solid Films*, vol. 520, no. 9, pp. 3609–3613, 2012.

[17] D. Dong, W. Wang, G. Dong et al., "Electrochromic properties and performance of NiO_x films and their corresponding all-thin-film flexible devices preparedby reactive DC magnetron sputtering," *Applied Surface Science*, vol. 383, pp. 49–56, 2016.

[18] I. Porqueras and E. Bertran, "Electrochromic behaviour of nickel oxide thin films deposited by thermal evaporation," *Thin Solid Films*, vol. 398-399, pp. 41–44, 2001.

[19] R. Lo Nigro, S. Battiato, G. Greco, P. Fiorenza, F. Roccaforte, and G. Malandrino, "Metal organic chemical vapor deposition of nickel oxide thin films for wide band gap device technology," *Thin Solid Films*, vol. 563, pp. 50–55, 2014.

[20] A. M. Soleimanpour, Y. Hou, and A. H. Jayatissa, "Evolution of hydrogen gas sensing properties of sol-gel derived nickel oxide thin film," *Sensors and Actuators, B: Chemical*, vol. 182, pp. 125–133, 2013.

[21] Y. Huang, Q. Zhang, J. Xi, and Z. Ji, "Transparent conductive p-type lithium-doped nickel oxide thin films deposited by pulsed plasma deposition," *Applied Surface Science*, vol. 258, no. 19, pp. 7435–7439, 2012.

[22] M. Li, X. Bo, Z. Mu, Y. Zhang, and L. Guo, "Electrodeposition of nickel oxide and platinum nanoparticles on electrochemically reduced graphene oxide film as a nonenzymatic glucose sensor," *Sensors and Actuators, B: Chemical*, vol. 192, pp. 261–268, 2014.

[23] D. Perednis and L. J. Gauckler, "Thin film deposition using spray pyrolysis," *Journal of Electroceramics*, vol. 14, no. 2, pp. 103–111, 2005.

[24] M. Jlassi, I. Sta, M. Hajji, and H. Ezzaouia, "Synthesis and characterization of nickel oxide thin films deposited on glass substrates using spray pyrolysis," *Applied Surface Science*, vol. 308, pp. 199–205, 2014.

[25] A. S. Enigochitra, P. Perumal, C. Sanjeeviraja, D. Deivamani, and M. Boomashri, "Influence of substrate temperature on structural and optical properties of ZnO thin films prepared by cost-effective chemical spray pyrolysis technique," *Superlattices and Microstructures*, vol. 90, pp. 313–320, 2016.

[26] F. A. Garcés, N. Budini, J. A. Schmidt, and R. D. Arce, "Highly doped ZnO films deposited by spray-pyrolysis. design parameters for optoelectronic applications," *Thin Solid Films*, vol. 605, pp. 149–156, 2016.

[27] P. C. Yu, G. Nazri, and C. M. Lampert, "Spectroscopic and electrochemical studies of electrochromic hydrated nickel oxide films," *Solar Energy Materials*, vol. 16, no. 1-3, pp. 1–17, 1987.

[28] P. Baraldi, G. Davolio, G. Fabbri, and T. Manfredini, "A spectral and thermal study on nickel(II) hydroxydes," *Materials Chemistry and Physics*, vol. 21, no. 5, pp. 479–493, 1989.

[29] A. Rahdar, M. Aliahmad, and Y. Azizi, "NiO nanoparticles: synthesis and characterization," *Journal of Nanostructures*, vol. 5, no. 2, pp. 145–151, 2015.

[30] P. V. Kamath and G. N. Subbanna, "Electroless nickel hydroxide: synthesis and characterization," *Journal of Applied Electrochemistry*, vol. 22, no. 5, pp. 478–482, 1992.

[31] R. Cerc Korošec, P. Bukovec, B. Pihlar, A. Šurca Vuk, B. Orel, and G. Dražič, "Preparation and structural investigations of electrochromic nanosized NiO_x films made via the sol-gel route," *Solid State Ionics*, vol. 165, no. 1-4, pp. 191–200, 2003.

[32] A. Lagashetty, V. Havanoor, S. Basavaraja, S. D. Balaji, and A. Venkataraman, "Microwave-assisted route for synthesis of

nanosized metal oxides," *Science and Technology of Advanced Materials*, vol. 8, no. 6, pp. 484–493, 2007.

[33] Y. Wang, J. Zhu, X. Yang, L. Lu, and X. Wang, "Preparation of NiO nanoparticles and their catalytic activity in the thermal decomposition of ammonium perchlorate," *Thermochimica Acta*, vol. 437, no. 1-2, pp. 106–109, 2005.

[34] A. S. Adekunle, J. A. O. Oyekunle, O. S. Oluwafemi et al., "Comparative catalytic properties of $Ni(OH)_2$ and NiO nanoparticles towards the degradation of nitrite (NO_2^-) and nitric oxide (NO)," *International Journal of Electrochemical Science*, vol. 9, no. 6, pp. 3008–3021, 2014.

[35] K. Sajilal and A. Moses Ezhil Raj, "Effect of thickness on physico-chemical properties of p-NiO (bunsenite) thin films prepared by the chemical spray pyrolysis (CSP) technique," *Optik*, vol. 127, no. 3, pp. 1442–1449, 2016.

[36] P. Oliva, J. Leonardi, J. F. Laurent et al., "Review of the structure and the electrochemistry of nickel hydroxides and oxy-hydroxides," *Journal of Power Sources*, vol. 8, no. 2-3, pp. 229–255, 1982.

[37] A. Al-Hajry, A. Umar, M. Vaseem et al., "Low-temperature growth and properties of flower-shaped β- $Ni(OH)_2$ and NiO structures composed of thin nanosheets networks," *Superlattices and Microstructures*, vol. 44, no. 2, pp. 216–222, 2008.

[38] X. Song and L. Gao, "Facile synthesis of polycrystalline NiO nanorods assisted by microwave heating," *Journal of the American Ceramic Society*, vol. 91, no. 10, pp. 3465–3468, 2008.

[39] F. Davar, Z. Fereshteh, and M. Salavati-Niasari, "Nanoparticles Ni and NiO: synthesis, characterization and magnetic properties," *Journal of Alloys and Compounds*, vol. 476, no. 1-2, pp. 797–801, 2009.

[40] D. M. Fernandes, A. A. W. Hechenleitner, M. F. Silva et al., "Preparation and characterization of NiO, Fe_2O_3, $Ni_{0.04}Zn_{0.96}O$ and $Fe_{0.03}Zn_{0.97}O$ nanoparticles," *Materials Chemistry and Physics*, vol. 118, no. 2-3, pp. 447–452, 2009.

[41] N. S. Das, B. Saha, R. Thapa, G. C. Das, and K. K. Chattopadhyay, "Band gap widening of nanocrystalline nickel oxide thin films via phosphorus doping," *Physica E: Low-Dimensional Systems and Nanostructures*, vol. 42, no. 5, pp. 1377–1382, 2010.

[42] A. C. Sonavane, A. I. Inamdar, P. S. Shinde, H. P. Deshmukh, R. S. Patil, and P. S. Patil, "Efficient electrochromic nickel oxide thin films by electrodeposition," *Journal of Alloys and Compounds*, vol. 489, no. 2, pp. 667–673, 2010.

[43] K. Ashok, "Characterization of nickel oxide thin film - DC reactive magnetron sputtering," *Surface Review and Letters*, vol. 18, no. 1-2, pp. 11–15, 2011.

[44] M. Alagiri, S. Ponnusamy, and C. Muthamizhchelvan, "Synthesis and characterization of NiO nanoparticles by sol-gel method," *Journal of Materials Science: Materials in Electronics*, vol. 23, no. 3, pp. 728–732, 2012.

[45] S. V. Ganachari, R. Bhat, R. Deshpande, and A. Venkataraman, "Synthesis and characterization of nickel oxide nanoparticles by self-propagating low temperature combustion method," *Recent Research in Science and Technology*, vol. 4, no. 4, 2012.

[46] L. G. Teoh and K.-D. Li, "Synthesis and characterization of NiO nanoparticles by solgel method," *Materials Transactions*, vol. 53, no. 12, pp. 2135–2140, 2012.

[47] D. Devadatha and R. Raveendran, "Structural and dielectric characterization of nickel-cobalt oxide nanocomposite," *Journal of Material Science & Engineering*, no. S-11, 2013.

[48] W. Yuan, F. Liu, and Z. Zhang, "Preparation and characterization of mesoporous Nickel oxide templated by different mixed surfactants," *Chinese Journal of Inorganic Chemistry*, vol. 29, no. 4, pp. 803–809, 2013.

[49] A. E.-A. A. Said, M. M. A. El-Wahab, S. A. Soliman, and M. N. Goda, "Synthesis and characterization of nano CuO-NiO mixed oxides," *Nanoscience and Nanoengineering*, vol. 2, no. 1, pp. 17–28, 2014.

[50] P. Godse, S. Sakhare, M. Pawar et al., "Effect of annealing on structural, morphological, electrical and optical studies of nickel oxide thin films," *Journal of Surface Engineered Materials and Advanced Technology*, vol. 1, no. 2, pp. 35–41, 2011.

[51] I. Van De Polluenten and I. Des Polluants, "projekt zee projet mer".

[52] J. Wang, P. Yang, X. Wei, and Z. Zhou, "Preparation of NiO two-dimensional grainy films and their high-performance gas sensors for ammonia detection," *Nanoscale Research Letters*, vol. 10, no. 1, pp. 1–6, 2015.

[53] H.-L. Chen, Y.-M. Lu, and W.-S. Hwang, "Effect of film thickness on structural and electrical properties of sputter-deposited nickle oxide films," *Materials Transactions*, vol. 46, no. 4, pp. 872–879, 2005.

[54] B. Cullity and S. Stock, *Principles of X-Ray Diffraction*, Addison-Wesley, Mass, USA, 1978.

[55] A. S. Riad, S. A. Mahmoud, and A. A. Ibrahim, "Structural and DC electrical investigations of ZnO thin films prepared by spray pyrolysis technique," *Physica B: Condensed Matter*, vol. 296, no. 4, pp. 319–325, 2001.

[56] M. Mekhnache, A. Drici, L. Saad Hamideche et al., "Properties of ZnO thin films deposited on (glass, ITO and ZnO:Al) substrates," *Superlattices and Microstructures*, vol. 49, no. 5, pp. 510–518, 2011.

[57] D. P. Padiyan, A. Marikani, and K. R. Murali, "Influence of thickness and substrate temperature on electrical and photoelectrical properties of vacuum-deposited CdSe thin films," *Materials Chemistry and Physics*, vol. 78, no. 1, pp. 51–58, 2003.

[58] N. Khedmi, M. Ben Rabeh, and M. Kanzari, "Structural morphological and optical properties of $SnSb_2S_4$ thin films grown by vacuum evaporation method," *Journal of Materials Science and Technology*, vol. 30, no. 10, pp. 1006–1011, 2014.

[59] A. S. a. P. S. Kumar, "Synthesis and characterization of NiO-ZnO nano composite," *Nano Vision*, vol. 1, no. 3, pp. 112–115, 2011.

[60] M. El-Kemary, N. Nagy, and I. El-Mehasseb, "Nickel oxide nanoparticles: synthesis and spectral studies of interactions with glucose," *Materials Science in Semiconductor Processing*, vol. 16, no. 6, pp. 1747–1752, 2013.

[61] W. O. George and P. S. McIntyre, *Infrared Spectroscopy*, John Wiley & Sons, Inc, NJ, USA, 1987.

[62] S. Benramache and B. Benhaoua, "Influence of substrate temperature and Cobalt concentration on structural and optical properties of ZnO thin films prepared by Ultrasonic spray technique," *Superlattices and Microstructures*, vol. 52, no. 4, pp. 807–815, 2012.

[63] H. C. Casey Jr., D. D. Sell, and K. W. Wecht, "Concentration dependence of the absorption coefficient for n- and p-type GaAs between 1.3 and 1.6 eV," *Journal of Applied Physics*, vol. 46, no. 1, pp. 250–257, 1975.

[64] R. Y. Mohammed, S. Abduol, and A. M. Mousa, "Correlation between optical and structural properties of chemically deposited cds thin films," *International Letters of Chemistry, Physics and Astronomy*, vol. 11, pp. 146–158, 2014.

[65] J. Tian, H. Deng, L. Sun, H. Kong, P. Yang, and J. Chu, "Effects of Co doping on structure and optical properties of TiO_2 thin

films prepared by sol-gel method," *Thin Solid Films*, vol. 520, no. 16, pp. 5179–5183, 2012.

[66] J. Tauc, R. Grigorovic, and A. Vancu, "Optical properties and electronic structure of amorphous germanium," *Phys Status Solidi B*, vol. 15, no. 2, pp. 627–637, 1966.

[67] J. D. Desai, S.-K. Min, K.-D. Jung, and O.-S. Joo, "Spray pyrolytic synthesis of large area NiO_x thin films from aqueous nickel acetate solutions," *Applied Surface Science*, vol. 253, no. 4, pp. 1781–1786, 2006.

[68] H. A. Juybari, M.-M. Bagheri-Mohagheghi, and M. Shokooh-Saremi, "Nickel-lithium oxide alloy transparent conducting films deposited by spray pyrolysis technique," *Journal of Alloys and Compounds*, vol. 509, no. 6, pp. 2770–2775, 2011.

[69] F. Urbach, "The long-wavelength edge of photographic sensitivity and of the electronic absorption of solids," *Physical Review*, vol. 92, no. 5, pp. 1324–1325, 1953.

[70] S. L. S. Rao, G. Ramadevudu, M. Shareefuddin, A. Hameed, M. N. Chary, and M. L. Rao, "Optical properties of alkaline earth borate glasses," *International Journal of Engineering, Science and Technology*, vol. 4, no. 4, pp. 25–35, 2013.

[71] K. J. Han, K. S. Kang, Y. Chen, K. H. Yoo, and J. Kim, "Effect of annealing temperature on the conduction mechanism for a sol-gel driven ZnO Schottky diode," *Journal of Physics D: Applied Physics*, vol. 42, no. 12, Article ID 125110, 2009.

[72] P. Mohanty, C. Rath, P. Mallick, R. Biswal, and N. C. Mishra, "UV-visible studies of nickel oxide thin film grown by thermal oxidation of nickel," *Physica B: Condensed Matter*, vol. 405, no. 12, pp. 2711–2714, 2010.